

# Determination of fracture toughness parameter of quasi-brittle materials with laboratory-size specimens

C. K. Y. LEUNG, V. C. LI

*Department of Civil Engineering, Massachusetts Institute of Technology, Cambridge, MA 02139*

An experimental technique based on four-point bend specimens has been developed for indirect determination of the tension-softening curve, which is suggested to be a size-independent fracture 'parameter' for quasi-brittle materials. The technique was applied to fibre-reinforced mortar. Good agreement between results from this indirect test and those from the direct tension test was obtained.

## 1. Introduction

For quasi-brittle materials such as concrete and rock, cracking is the major cause of material failure in many cases. As a result, assessment of the resistance to crack propagation would be crucial in the understanding of behaviour of structures involving such materials. In other words, the determination of a fracture toughness parameter of the materials becomes very important.

Earlier investigations in the fracture of quasi-brittle materials assume the validity of linear-elastic fracture mechanics (LEFM) for the laboratory specimens employed and LEFM toughness parameters such as  $K_{Ic}$  and  $G_{Ic}$  are determined. However, such parameters as obtained from normal laboratory sized specimens are found to be dependent on the specimen size. The size dependence is due to the presence of a large planar process zone in front of the crack tip where micro-cracking and aggregate pull-out lead to softening behaviour. For LEFM to be valid, the size of this process zone should be small compared to other characteristic planar dimensions of the specimen to satisfy the so-called small scale yielding criteria. However, large process zone size observed or estimated in concrete and cement composites often invalidates LEFM based fracture toughness tests. As a result, very large specimens are required to obtain the true  $K_{Ic}$  value. This fact is well documented in the literature. For example, Francois [1] summarized reported  $K_{Ic}$  values for concrete obtained with various specimen sizes and found that  $K_{Ic}$  increased with specimen size and became constant only when the specimen size is over 1 meter (Fig. 1). Hillerborg [2] argued that LEFM was applicable only when both the crack size and the ligament size were greater than  $2-5l_{ch}$ , where  $l_{ch} = EG_c/f_t^2$  was a characteristic length of the material. For concrete, typical values for  $l_{ch}$  are 200-400 mm, hence a minimum specimen size of 1.5-2 m is required. For steel-fibre reinforced concrete,  $l_{ch}$  can range from 2-20 m and specimen size of at least 10 m

is required. Such specimen sizes are clearly impractical in the laboratory.

The tension-softening ( $\sigma$ - $\delta$ ) relation (Fig. 2) is defined as the functional relationship between the traction across a crack plane and the separation distance of the crack faces in a uniaxial tension specimen quasi-statically loaded to complete failure. The  $\sigma$ - $\delta$  relation gives us several pieces of useful information. The maximum stress value is simply the tensile strength  $f_t$ . The maximum value of  $\delta$  is the critical separation of the material, the separation beyond which the material becomes part of the 'real crack', where there is no traction acting between the opposite faces. The area of the curve can be interpreted as  $J_c$  for the material. This is equivalent to the critical energy release rate  $G_c$  under small scale yielding condition.  $G_c$  is related to  $K_{Ic}$  through the equation  $G_c = K_{Ic}^2/E$  (for plane stress conditions). Hence, from the area of the tension-softening relation, the LEFM fracture parameters can be obtained. Moreover, the  $\sigma$ - $\delta$  relation can be employed to extend fracture analysis to cases when LEFM is inapplicable. Li and Liang [3] describe the transition of validity of LEFM to non-linear elastic fracture mechanics to simple strength concept through the  $\sigma$ - $\delta$  relation and show how the shape of the  $\sigma$ - $\delta$  curve can affect structural behaviour. Ingraffea and Gerstle [4] used the  $\sigma$ - $\delta$  relation in their finite element code and carried out nonlinear fracture mechanics analysis to study the propagation of cracks. Hence, the  $\sigma$ - $\delta$  relation is a very useful basic 'parameter' for fracture characterization of quasi-brittle materials that exhibit tension-softening behaviour.

By definition, the tension-softening relation can be obtained directly from a tensile test. However, a major problem with the direct tensile test is the stability of loading the specimen in the softening regime. Attempts at measuring the  $\sigma$ - $\delta$  relation through the use of stiffened machine [5, 6] and feedback control loop [7, 8] have been met with various successes. However,

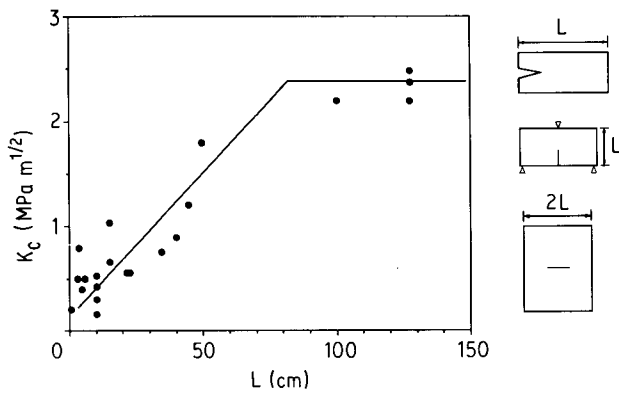


Figure 1 Various results of the fracture toughness  $K_c$  as a function of the size of the specimen (taken from current literature).

problems related to load eccentricity, crack location(s), effects of strain gauge length and elastic unloading still exist and make the test difficult to perform. Moreover, the modifications on the testing machine are too complicated for such testing methods to be widely adopted in normal testing laboratories.

Li [9] has suggested an experimental technique based on the  $J$ -integral to obtain the  $\sigma$ - $\delta$  relation in an indirect way. Li, Chan and Leung [10] described the technique in detail and applied it to plain mortar using the compact tension specimen geometry. The  $\sigma$ - $\delta$  curve obtained was in good qualitative agreement with those reported in the literature.

The objective of the present investigation is to develop the above mentioned indirect experimental technique for the four-point bend specimen geometry, with application to general quasi-brittle materials and particularly fibrous composites. To verify the validity of this indirect technique, steel-fibre reinforced mortar, a material with reported tension-softening relation obtained by direct tension test, was used so that comparison of our results with those from direct tests can be made.

In this account, the theory is first briefly summarized. Then specimen preparation and the experimental set up will be described in detail. Data analysis procedures and results are then reported followed by comparison with other test results and discussion. Good agreements between results from this indirect technique and those from direct tensile test give us confidence in further application of this technique to cementitious composites with other kinds of fibres as

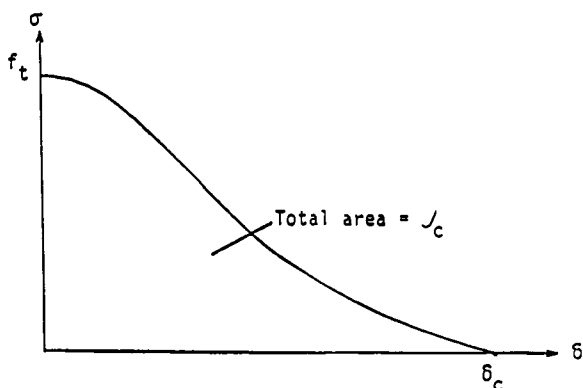


Figure 2 A typical tension-softening curve.

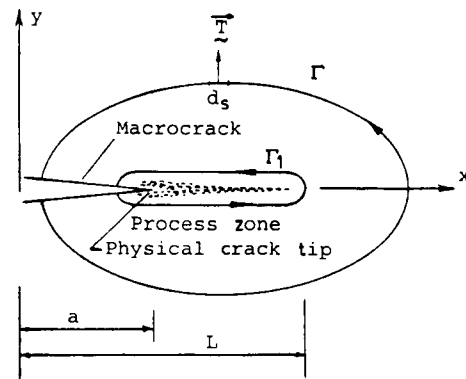


Figure 3  $J$ -integral contours around crack tip.

well as other quasi-brittle materials such as rock and ceramics.

## 2. A brief summary of the theoretical basis

The theory is more thoroughly explained in [10] to which the interested reader is referred. Here, only a brief summary will be given for completeness.

The  $J$ -integral introduced by Rice [11], if evaluated for a contour  $\Gamma$  running alongside the process zone (Fig. 3) can be expressed as:

$$J(\delta) = \int_0^\delta \sigma(\delta) d\delta \quad (1)$$

where  $\delta$  is the separation at the physical crack tip.

$J$  can be obtained experimentally from a compliance test by loading two precracked specimens with slightly different crack lengths. If the load  $P$ , the load point displacement  $\Delta$  and the crack tip separation  $\delta$  are measured simultaneously in the test,  $J$  can be first obtained in terms of  $\Delta$  from the area  $A(\Delta)$  between the two  $P$ - $\Delta$  curves up to a load point displacement value of  $\Delta$ .

$$J(\Delta) = (1/B)[A(\Delta)/(a_2 - a_1)] \quad (2)$$

where  $B$  is the width of the specimen and  $(a_2 - a_1)$  is the difference in crack length.  $J(\Delta)$  can then be converted to  $J(\delta)$ .

By differentiating Equation 1, we have

$$\sigma(\delta) = \partial J(\delta) / \partial \delta \quad (3)$$

which is the tension-softening relation of the material.

Theoretically,  $(a_2 - a_1)$  should be as small as possible but experimental accuracy and material variability put a lower limit on this value.

## 3. Numerical verification of testing procedure

An independent verification for our testing procedure was provided by A. Hillerborg (private communications, 1985). He employed his fictitious crack model in a finite element scheme to simulate the load-load point displacement curves and load-crack tip separation curves of a pair of three point bend specimens of slightly different notch lengths. He used an artificial bi-linear curve as input for the tension-softening behaviour in the material ahead of the notches. The objective of the exercise is to extract this same curve using the indirect technique described in the last

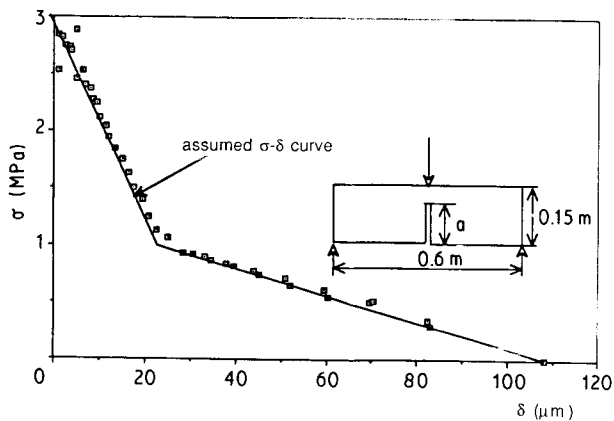


Figure 4 Assumed bi-linear and computed tension-softening curve (Hillerborg, personal communication, 1985).  $E = 30000 \text{ MPa}$ ,  $G_F = 90 \text{ nm}^{-1}$ ,  $F_t = 3 \text{ MPa}$  and  $a = (0.0525 \text{ m})(0.05625 \text{ m})$ .  $\square$  = numerically computed base on  $J$ -integral procedure.

section and his numerically derived 'test' results. If the  $J$ -integral based test technique is theoretically sound, then he should get a predicted tension-softening curve overlapping the bi-linear curve he inputted into his finite-element program. The result is most encouraging. As shown in Fig. 4, the two curves essentially overlap one another.

#### 4. Specimen specification and preparation

In previous investigations of this indirect technique [10], compact tension specimens have been used. In the present investigation, four-point bending specimens are employed. The bending specimen has the following advantages:

1. The compact tension specimen has an unbalanced configuration. It is necessary to attach a balance weight to it at the start of the test. The bending specimen, which is a self-balanced configuration is thus preferred.
2. The bending specimen has been widely used by the concrete and rock testing community and details concerning its sources of errors and their effect on the

accuracy are well documented (for example, Baretta [12]).

The four-point bending configuration is chosen because it gives a uniform moment at the central span which does not give rise to any shear stress at the crack plane.

The material used is 1 : 2 : 0 : 0.5 mortar reinforced with 1 vol % of steel fibre. The mortar is Type III portland cement. The aggregate is sieved before use so that the maximum sized aggregate pass through a No. 8 screen. The fibre is 9.525 mm hot-melted steel fibre supplied by Ribtec Inc. (Gahanna, OH, USA). The cross-section of the fibre is of an irregular shape and the cross-sectional area varies along the fibre length. The effective diameter specified by the manufacturer is 0.1524 mm.

In the mixing procedure, an aggregate was first added into the mixer with a small portion of the water. Fibres were then added through a sieve to ensure proper dispersion. After all the fibres were added, cement was added in with the remaining water. The contents were then mixed for three minutes, left covered in the mixer for three minutes and then mixed for a final two minutes.

After mixing, the material was put into the moulds. Two kinds of specimens were prepared – bending specimens and direct tension specimens. The mould for the bending specimen is shown in Fig. 5. The beam size is  $431.8 \times 114.3 \times 63.5 \text{ mm}$ . Steel bars were stuck onto the mould with double sided tape before pouring in the concrete so that they would be casted in the final specimens. The steel bars are at the position of the load application points as well as the support points. Hence, they serve to reduce the crushing of concrete which tends to dissipate energy at such points of stress concentration. On the upper steel bars (where the load application points are), screw holes are drilled so that posts can be put in to support a target plate for the measurement of vertical displacement at the load points (refer to Fig. 8). For stability, the (crack depth/beam depth) ratio should not be too small. A ratio higher than about 0.4 seems good enough. A thorough

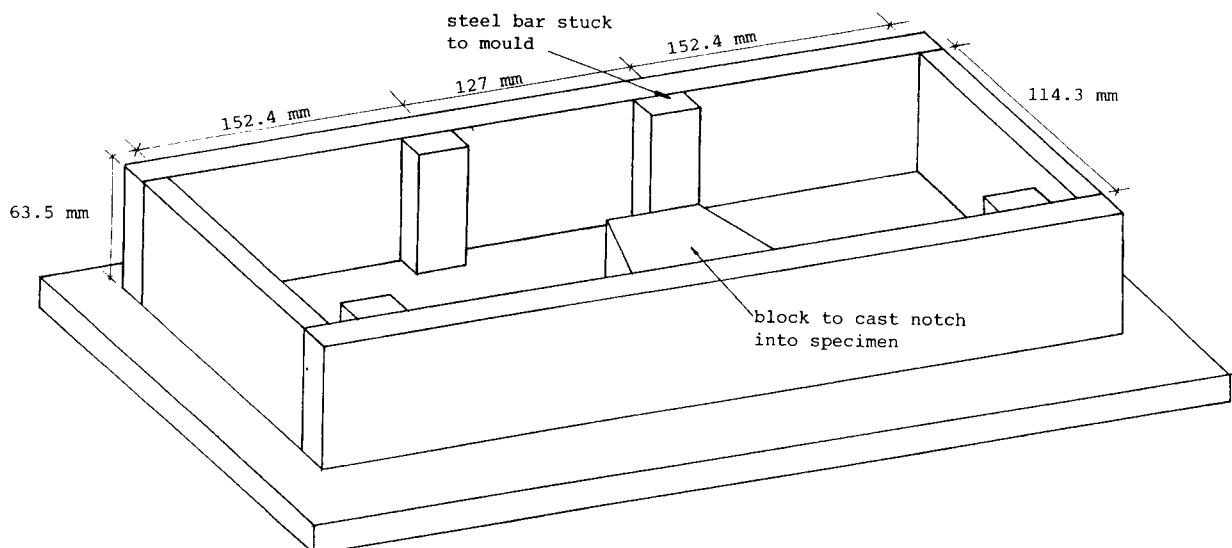


Figure 5 Mould for the bending specimen. Inner dimensions:  $431.8 \text{ mm}$  (length)  $\times$   $114.3 \text{ mm}$  (breadth)  $\times$   $63.5 \text{ mm}$  (depth) (Note that during testing the "breadth" direction is vertical). Size of trapezoidal block  $50.8 \text{ mm}$  (top)  $76.2 \text{ mm}$  (bottom)  $31.75$  (height).

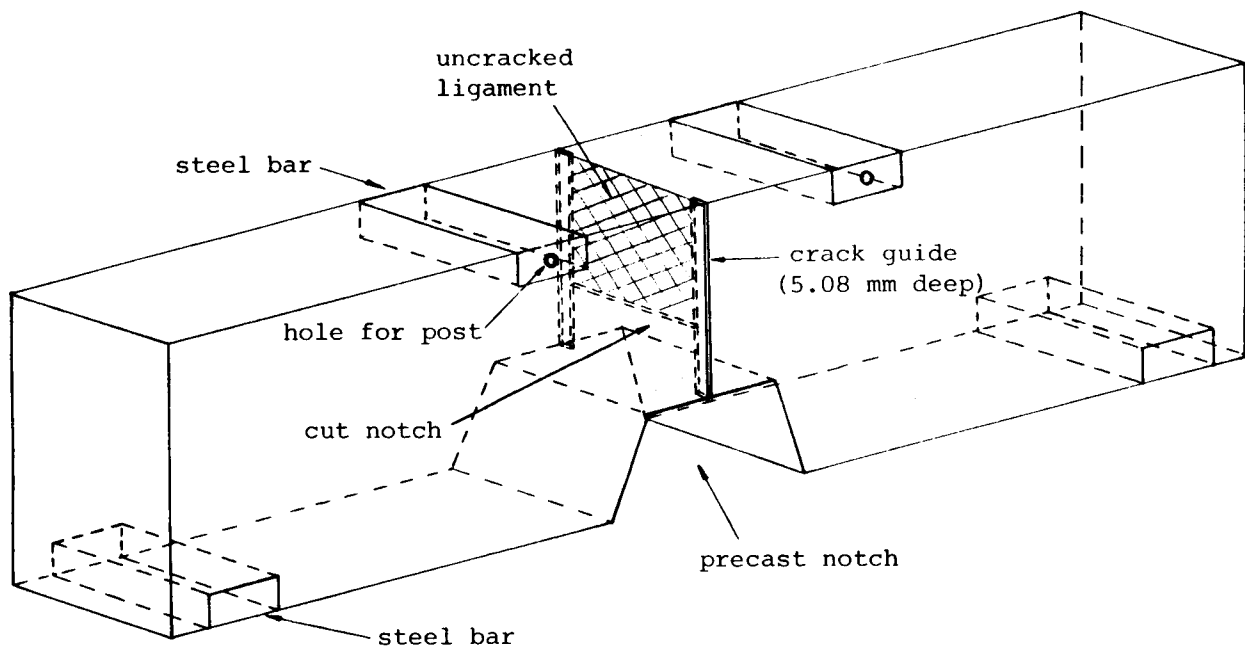


Figure 6 A bending specimen ready for testing.

discussion on the stability criteria for bending specimens is found in Petersson [13]. The cast-in trapezoidal notch of 31.75 mm depth is to reduce the length of crack that has to be cut by saw after the concrete has stiffened. All together, eight bending specimens were prepared so that four specimens were tested for each crack length.

The direct tension specimens are 128 mm long with a square cross-section of  $50.8 \times 50.8$  mm. They were cast with the long side horizontal so that the fibre distribution should be similar to the bending specimen. Three specimens were prepared for the tensile test.

Both kinds of specimens were cast in two layers with each layer vibrated for about one minute on the vibrating table. To avoid fibre disturbance, no rodding was attempted. The specimens were covered with plastic-wrap for one day and then cured in water with a small amount of cement to give some alkalinity. After curing for 4 more days, the specimens were taken out of water.

For the bending specimens notches were cut with a diamond saw. Depth of the cut was 12.7 mm for four of them and 22.86 mm for the other four (i.e. the total notch depth with the precast trapezoidal notch are 44.45 mm and 54.61 mm respectively). Also, two crack guides along full ligament of 5.08 mm depth each were cut at the two sides of the specimen vertically upwards from the cut notches to make sure that the crack propagates in the vertical plane. A specimen ready for test is shown in Fig. 6.

The tension specimens would be tested in direct tension to obtain the tensile strength of the material for comparison with the value obtained indirectly on the tension-softening curve. Since only the peak strength is required, we do not have to worry about the post-peak instability. A set-up designed by Soon [14] is employed. The prismatic specimens were glued with epoxy to two end plates. Weights were then put on top and the specimens left for at least 48 hours for the epoxy to gain strength before testing.

Both the bending specimens and direct tension specimens were tested at an age of seven days.

## 5. Experimental procedure and instrumentation

The bending specimen is put on two supports 381 mm apart. The load application points are 127 mm apart equidistant from the plane of the pre-cut notch. Loading was applied through two curved surfaces below a loading plate. The curved surfaces are connected to the loading plate by a rod at one side and a ball at the other side to eliminate torsion. A spherical seat with a socket is placed at the center of the loading plate to ensure that the applied force is vertical. The supports are also curved surfaces attached to the support blocks by rod at one side and by a ball on the other side.

In the bending test, the load, load point displacement and crack tip separation are measured simultaneously. At the crack tip, a non-contacting proximity sensor which can measure up to 0.254 mm is used in parallel with a linear variable displacement transducer (LVDT) that can measure up to 5.08 mm (Fig. 7). In this case, the LVDT is used in a horizontal position

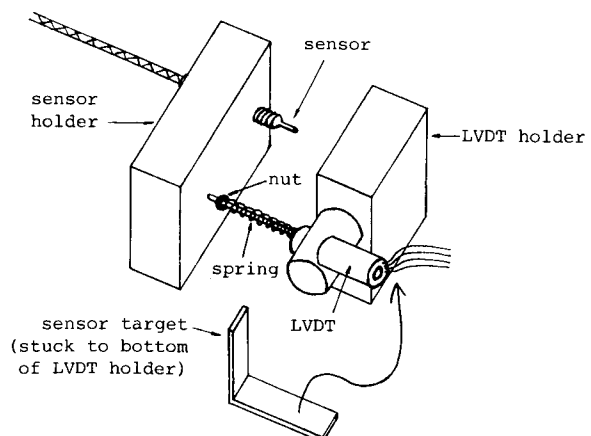


Figure 7 Instrumentation for the measurement of the crack tip separation.

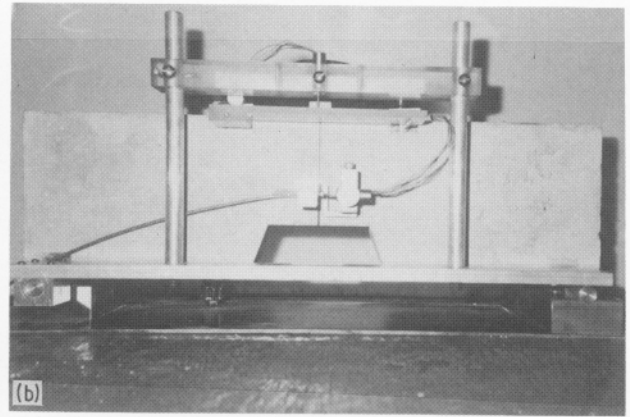
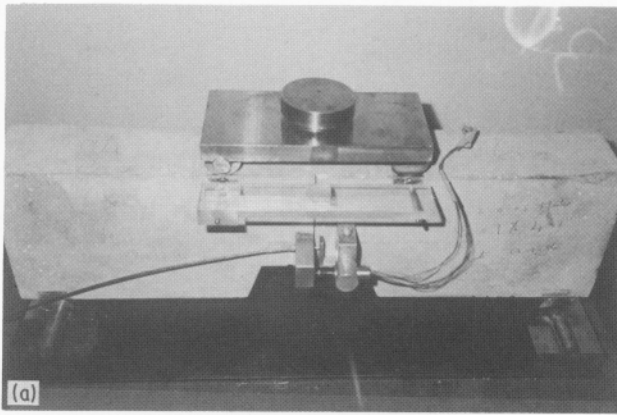


Figure 8 (a) Experimental apparatus (without the vertical LVDT and its holder); (b) Experimental apparatus (with the vertical LVDT and its holder).

with its shaft held against the target by a spring. Under such a situation, it is very difficult to ensure that the shaft is perfectly horizontal and thus hard to get an accurate calibration factor for the LVDT. On the other hand, the calibration factor of the sensor will not change with orientation. Thus, at the early stage of the test, readings are taken with both the sensor and the LVDT and regression is done on the two sets of data to obtain a calibration factor for the LVDT. This factor will then be used for all readings taken with the LVDT when the sensor goes out of range.

For the measurement of vertical displacement, the LVDT is put vertically on its holder. In this case, the shaft will be vertical due to gravity and hence we do not need to use the LVDT with a sensor. The holder for the vertical LVDT is held in such a way that it moves with the supports of the specimen so even if the support blocks settle, our results will not be affected. Photographs of the set-up are shown in Figs. 8a and 8b.

The bending test is carried out in an Instron (Instron Corp., Canton, MA, USA) loading frame. Signal outputs from the LVDTs, the sensors as well as the load cell of the loading frame are recorded by a Fluke (J. Fluke, Everett, WA 98208) data acquisition system and sent immediately to an IBM PC where the data is stored. Computer programs are then written to transform the data into the required form and data is then transferred to a main frame computer for analysis and plotting.

From tension-softening curves reported in the literature, it is observed that the stress changes sharply with displacement at a small amount of separation. Once separation gets larger, the curve becomes flatter. Therefore, to capture the sharp change at the early stage of the test, when the separation is small, a slow loading rate has to be used. However, in order to

computer. Tensile force is applied through two steel strings, one at each end of the specimen. The maximum load is read directly as output on the micro-computer and the peak strength can be easily calculated. The loading rate for the tensile test is such that the peak is reached in about five minutes, while in the bending test, the peak load is reached within about ten minutes. In the bending test, the tensile strength of the material is reached before the structure reaches its peak load. By adjusting the loading rates as described above, the actual rate of loading of the material in the two testing configurations become comparable.

## 6. Results and data analysis

The raw data curves for  $P$  vs  $\Delta$  and  $\delta$  vs  $\Delta$  for each crack depth are shown in Fig. 9a, b and Fig. 10a, b. Four specimens were tested for each crack length and only the ones that seem to be consistent with each other were used in the analysis. In the present case, all the curves for  $a = 54.61$  mm are used. However, for  $a = 44.45$  mm, the curve showing the highest load in the  $P$  vs  $\Delta$  plot (Fig. 9a) is not used. This curve is rejected based on two reasons. Firstly, comparison with  $P$ - $\Delta$  curves for the same crack length shows that it deviates a great deal from the other curves. Secondly, examination of the broken specimens reveals that the specimen corresponding to this curve broke in an unexpected manner. After growing vertically for a while, the crack moved out of the crack guide and formed a large wedge on one side. This difference in crack propagation behaviour and the resulting  $P$ - $\Delta$  curve is probably due to non-uniform distribution of fibre in that particular specimen.

At the beginning of the test, there was some sitting problem at the supports which could not be eliminated completely. As a result, the  $P$  vs  $\Delta$  curve is not linear at the start. The curve is initially non-linear and

Figure 9 (a) Raw data curve for specimens with shorter precrack  $a = 44.45$  mm. (b) Raw data curve for specimens with longer precrack  $a = 54.61$  mm.

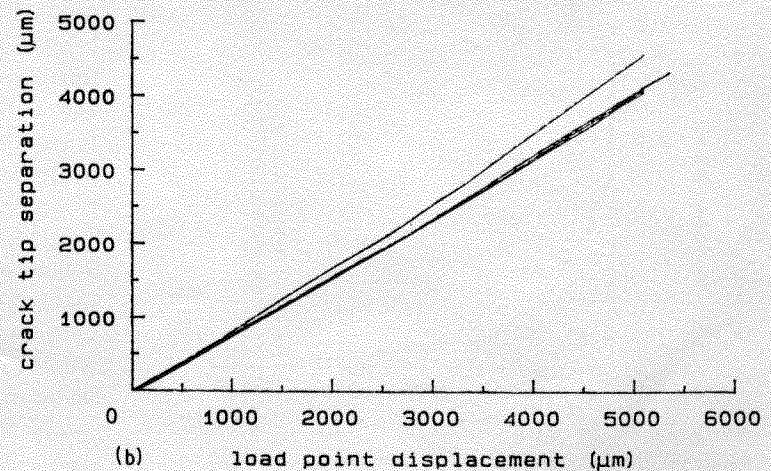
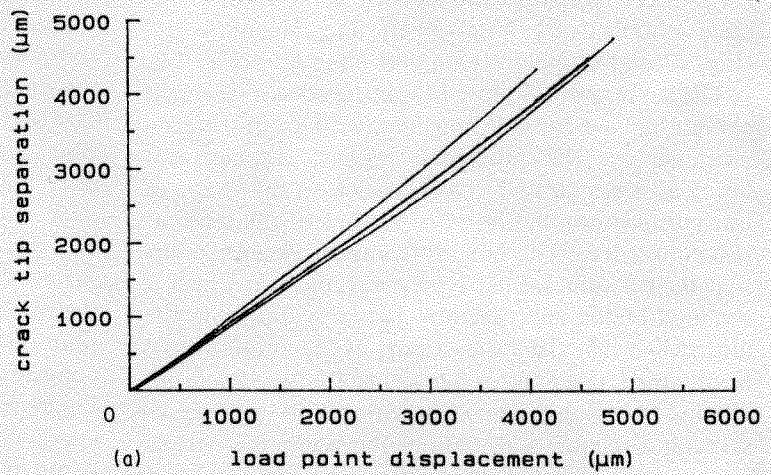
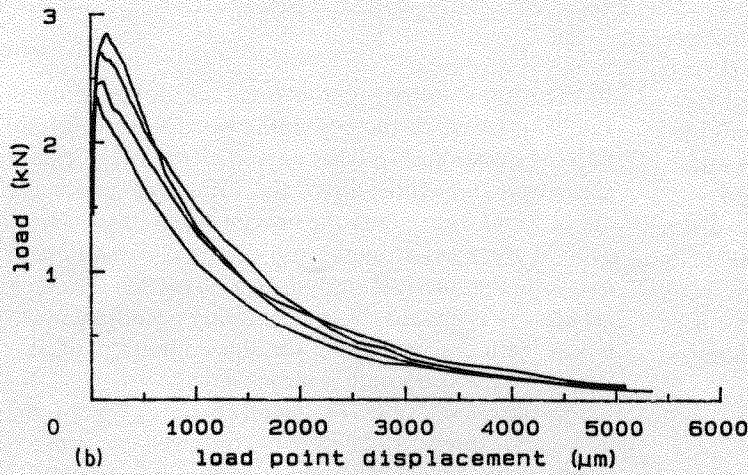
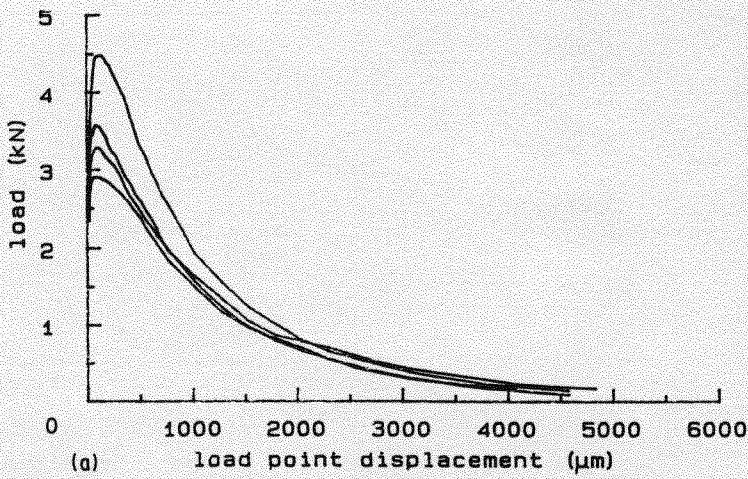


Figure 10 (a) Raw data curve for specimens with shorter precrack  $a = 44.45$  mm. (b) Raw data curve for specimens with longer precrack  $a = 54.61$  mm.

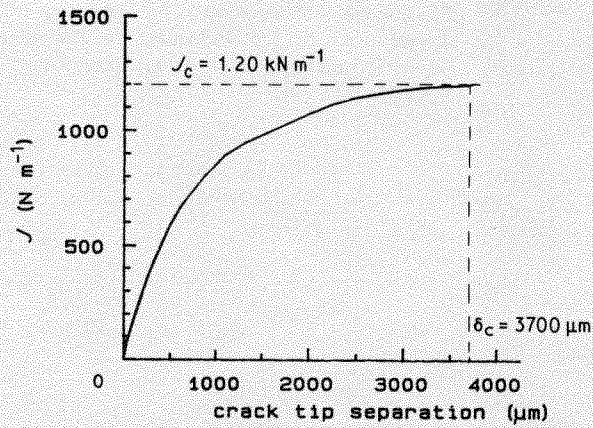


Figure 11  $J$  against crack tip separation curve.

respectively. At each  $\Delta$ , we compute  $J(\Delta)$  by numerical integration of  $P_1(\Delta) - P_2(\Delta)$  from  $\Delta' = 0$  to  $\Delta$  and divided by  $B(a_2 - a_1)$ . Also,  $\delta$  is obtained from  $(\delta_1(\Delta) + \delta_2(\Delta))/2$ . Hence, a  $J$ - $\delta$  curve can be obtained (Fig. 11). By numerical differentiation of this curve, the tension-softening curve (Fig. 12) is deduced.

The tensile strength obtained from three direct tension specimens has an averaged value of 3.004 MPa with a standard deviation of 0.1208 MPa. The peak value of 2.802 MPa obtained on the  $\sigma$ - $\delta$  curve is in reasonably good agreement with the direct tension test result.

## 7. Discussion

The deduced tension-softening curve from the indirect technique was compared qualitatively with curves from direct tensile test on steel fibre reinforced concrete obtained by Visalvanich and Naaman [15] (Fig. 13 and Gopolaratnam and Shah [16] (Fig. 14).

The curve shown in Fig. 13 was a load-displacement curve obtained for 6.35 mm fibre with an unstiffened machine. At the post-peak regime, displacement becomes concentrated at the crack and the shape of this curve is exactly the same as that of the tension-softening curve. The only difference between them is that their y-values differ by a constant ratio which is the area of the cross-section. It is obvious from the dotted line that the steepest part of the curve cannot be obtained, presumably due to instability. As a result of this, the loading becomes temporarily non-quasi-static and reliability of data at the beginning part of

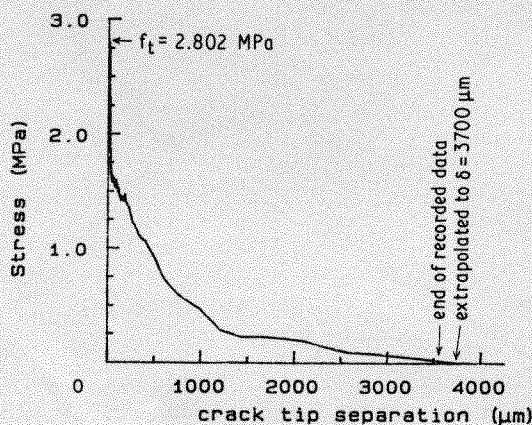


Figure 12 The deduced tension-softening curve.

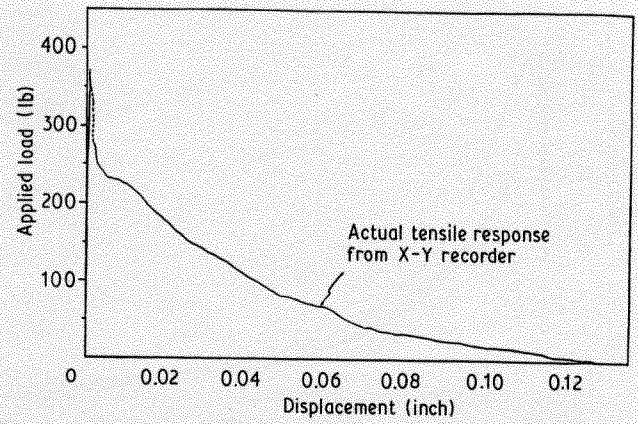


Figure 13 Typical tensile load against displacement curve of steel fibre reinforced mortar [15]  $V_f = 1\%$ , fibre length = 6.35 mm  $l/d = 42$ .

the tension-softening curve (i.e., the dotted part in Fig. 13 as well as the beginning portion of the solid part) is questionable. This part of the curve does not seem to significantly affect the total area under the curve which represents the energy release rate. However, if we want to make use of the  $\sigma$ - $\delta$  relation to carry out a numerical analysis in a case when the crack separation is limited (by serviceability requirement) to a low value, accuracy in the determination of this initial part will become important.

For the curve in Fig. 13 and all curves in Fig. 14, the  $\sigma$ - $\delta$  curve shows a sharp drop followed by a much more gentle slope. This is in qualitative agreement with the curve we obtained. However, since the slope at the flatter part is mainly governed by interfacial friction between the fibre and the matrix, quantitative comparisons cannot be made as both the fibres and the concrete composition are different between our case and theirs. Another point which can be observed when comparing Fig. 13 and our curve (Fig. 12) is that after the sharp drop, the stress drops slowly to zero in a more or less quadratic fashion. This is again evidence of a frictional process. In the case of uniformly distributed fibre, the number of fibres bridging the crack as well as the averaged length of the bridging fibre both varies linearly with crack separation. If a constant sliding friction is acting between the fibre and the matrix, a quadratic drop will be observed. In our curve, though the trend looks like quadratic, the curve is rather rugged. This is probably due to the use of a fibre with non-uniform shape in our composite which leads to a varying frictional force as well as ruggedness introduced through the numerical differentiation. In Fig. 14 the tension-softening curves appear to be more linear than those in Figs. 12 and 13 after the sharp drop from the peak. It has to be pointed out that this is due to the difference in scale of the curves. In Fig. 14, displacement is only measured up to about 260  $\mu\text{m}$  while in the other two investigations, displacement is measured to over 3000  $\mu\text{m}$ . Actually, if we concentrated on the initial parts of Figs. 12 and 13 where displacement is small, the curves also appear to be approximately linear.

The critical opening,  $\delta_c$  in our case, is extrapolated due to limited travel of the LVDT used from 3600  $\mu\text{m}$

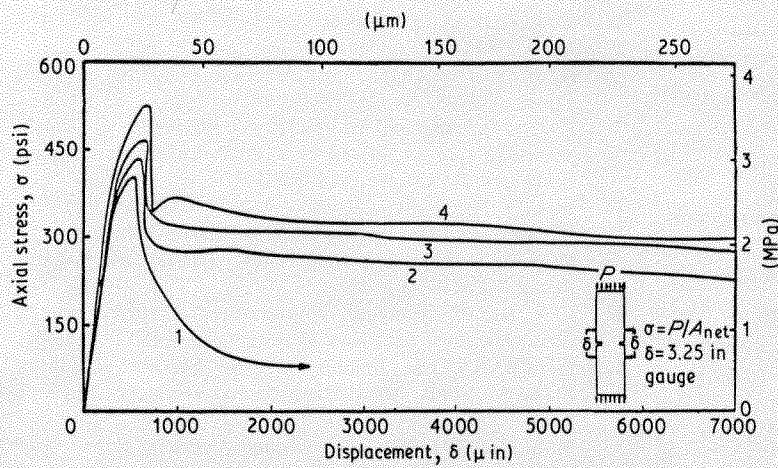


Figure 14 Typical results of tension-softening curves obtained from direct tension tests on plain mortar and SFRC containing 0.5, 1.0 and 1.53 vol % fibres respectively. Fibre length of 25.4 mm and 0.406 mm diameter were used for all the SFRC mixes [16] Key: 1. Plain mortar matrix; 1:2:0.5 (c:s:w); den specimen  $3 \times 3/4 \times 12$  in; net section  $2 \times 3/4$  in; notch width 0.1 in. 2.  $V_f = 0.5\%$ . 3.  $V_f = 1.0\%$ . 4.  $V_f = 1.5\%$ .

to  $3700 \mu\text{m}$ . Theoretically, for a uniform distribution of fibre, the longest pull-out length of the fibres is half of the fibre length. In other words, only after the separation gets beyond half the fibre length will all the fibres be pulled out and the stress drop to zero. Therefore,  $\delta_c$  should be half the fibre length or  $4762.5 \mu\text{m}$  in this case. One plausible explanation for the discrepancy is that the fibre we used is of non-uniform cross-sectional area along its length. The part with the largest cross-section is usually not at the end and after this part is pulled out, the remaining part offers little resistance since the track for it to move out is already widened and there is little interaction between the fibre and the matrix. This effect tends to reduce the value of  $\delta_c$  since the stress can drop to a very low value (not easy to be obtained experimentally) before all the fibres are actually pulled out.

From Fig. 11, we obtain  $J_c = 1.20 \text{ kN m}^{-1}$  for the material we used.  $J_c$  can also be obtained from the area of the tension-softening curve and so we estimate  $J_c$  from Fig. 13. From reference [15], the specimen used for the determination of Fig. 13 has a square cross-section of  $25.4 \times 25.4 \text{ mm}$  with a notch at midlength to confine cracking to one section. Neglecting the area of the notch we compute stress from load by dividing it with the total cross-sectional area. Then, from area of the stress-displacement curve,  $J_c$  is estimated to be  $1.87 \text{ kN m}^{-1}$ . Since different kinds of matrix material and fibre are used in our investigation and theirs, it is not possible to compare results directly (though, if we assume the same kinds of fibre and matrix, the  $J_c$  value from their result should be lower than ours because we are using a longer fibre with a higher aspect ratio). However, since the two  $J_c$  values are of the same order of magnitude, we can say that the  $J_c$  value we obtained is within a reasonable range.

In the data analysis, the tension-softening curve is obtained from numerical interpolation of raw data followed by numerical integration and differentiation. This procedure, though a convenient means, may lead to ruggedness of the curve. An alternative is to do a nonlinear regression on the data. A regressed expression of the  $J-\delta$  curve can then be differentiated analytically to get a smooth  $\sigma-\delta$  curve. This approach has been tried out but is not used in this paper. The tension-softening curve is dominated by different micro-mechanisms at various ranges giving rise to a

highly nonlinear curve with sharp changes in shape. Thus, a smooth function that can fit the entire range of data well is hard to find.

In this experimental technique, the sitting problem at the support requires linear extrapolation of data. Since the later analysis will be sensitive to the extrapolation result, the direct tensile test result becomes important in the sense that it provides a check for the accuracy of the extrapolation. If the tensile strength obtained on the  $\sigma-\delta$  curve agree well with that from the direct tensile test, the extrapolation can be considered accurate. On the other hand, we may have to re-extrapolate until we get a better agreement.

The  $P-\Delta$  curves in Fig. 9a and b appear to be quite smooth, showing that changes in loading rate during the test do not have any significant effect on our result.

The difference between the indirect technique we used here and the RILEM  $G_F$  test [17] is worth noting. In their test, pre-cracked specimens with only one crack size is needed and only the apparent critical energy release rate can be determined. In our test, two kinds of cracked specimens are used and we can obtain  $G_c$ ,  $\delta_c$  and also the shape of the  $\sigma-\delta$  curve. In other words, more information is provided by our test results. Also, it is thought that the value of  $G_c$  we obtain will be subject to a much smaller size dependence than the RILEM test value. The size dependence is mainly due to irrecoverable damages outside the cracking plane which tends to increase with the specimen size. More thorough discussions can be found in Li [9] and Jenq and Shah [18]. In our case,  $G_c$  is obtained from the difference in energy of two specimens with slightly different crack size. The irrecoverable losses will tend to compensate each other for the two specimens and hence the size dependence can be greatly reduced.

In conclusion an indirect experimental technique is developed to obtain the tension-softening curve of quasi-brittle materials. Four-point bending configuration is employed. The test involved only laboratory-sized specimens and can be easily performed without the need of modification of testing machines. The method is first applied to steel-fibre reinforced mortar for which reported tension-softening curves are available from the literature for comparison. Our results are found to be in good qualitative agreement with those obtained by a direct tensile test. The good



agreement gives us confidence in the application of this technique to other fibre-reinforced composites as well as other quasi-brittle materials such as rocks and ceramics.

### Acknowledgement

The authors would like to thank A. Hillerborg for performing the FEM numerical verification of the test technique. Supports from a grant (MSM-8516893) from the Solid and Geomechanics Program of the National Science Foundation and from a contract with the Shimizu Construction Company, Ltd. are gratefully acknowledged.

### References

1. D. FRANCOIS, "Applications of Fracture Mechanics to Cementitious Composites", Edited by S. P. Shah (Martinus Nijhoff Publishers, Dordrecht, 1985) p. 141.
2. A. HILLERBORG, "Fracture Mechanics of Concrete", Edited by F. H. Wittmann (Elsevier Science Publisher, B. V., Amsterdam, 1983) p. 223.
3. V. C. LI and E. LIANG, *ASCE J. Eng. Mech.* **112** (1986) 566.
4. A. R. INGRAFFEA and G. H. GERSTLE, "Applications of Fracture Mechanics to Cementitious Composites", Edited by S. P. Shah (Martinus Nijhoff Publishers, Dordrecht, 1985) p. 247.
5. R. H. EVANS and M. S. MARATHE, *Materieux et Constructions I* (1968) p. 61.
6. P. -E. PETERSSON, "Crack Growth and Development of Fracture Zones in Plain Concrete and Similar Materials", Report TVBM-1006, Lund Institute of Technology, Division of Building Materials (1981).
7. V. S. GOPALARATNAM and S. P. SHAH, *ACI Journal*, **82** (1985) p. 310.
8. H. W. REINHARDT, HERON, Delft University of Technology, Vol. 29, No (2) (1984).
9. V. C. LI, "Applications of Fracture Mechanics to Cementitious Composites", Edited by S. P. Shah (Martinus Nijhoff Publishers, Dordrecht, 1985) p.431.
10. V. C. LI, C. M. CHAN and C. K. Y. LEUNG, "Experimental Determination of the Tension-Softening Relations for Cementitious Composites", *Cement and Concrete Research* **17** (1987) p. 441.
11. J. R. RICE, "Fracture: An advanced Treatise", Vol. 2 (Academic Press Inc., New York (1968) p. 191.
12. F. I. BARATTA, Requirements for Flexure Testing of Brittle Materials, Army Materials and Mechanics Research Center, TR 82-20 (1982).
13. P. -E PETERSSON, *Cement and Concrete Research* **10** (1980) p. 78.
14. K. A. SOON, Behaviour of Pressure Confined Concrete in Monotonic and Cyclic Loading, Ph.D Thesis, Department of Civil Engineering, M.I.T (1987).
15. K. VISALVANICH and A. NAAMAN, *ACI Journal* **80** (1983) p. 128.
16. V. S. GOPOLARATNAM and S. P. SHAH, *ASCE J. Eng. Mech.* **113** (1987) p. 635.
17. Proposed RILEM Recommendation, Determination of the Fracture Toughness of Mortar and Concrete by Means of Three Point Bend Tests on Notched Beams, Division of Building Materials, Lund Institute of Technology, Lund, Sweden (1982).
18. Y. S. JENQ and S. P. SHAH, "Applications of Fracture Mechanics to Cementitious Composites", Edited by S. P. Shah (Martinus Nijhoff Publishers, Dordrecht, 1985). p. 319.

Received 18 August 1987  
and accepted 21 March 1988